# Mapping offset channels from LiDAR derived terrain models along Hunter Mountain Fault Zone.

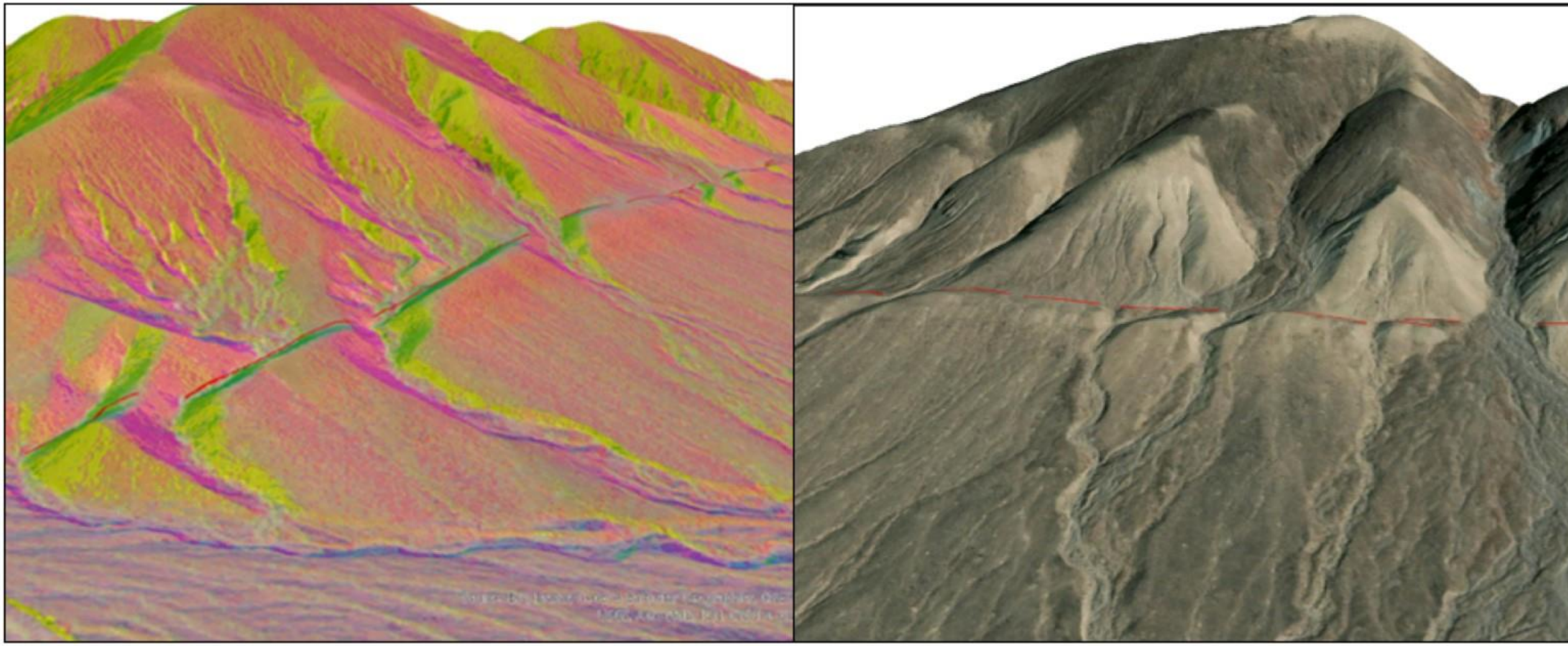

Timothy Randol

GEOG 593: Digital Terrain Analysis

Portland State University

Fall 2020

# Mapping offset channels from LiDAR derived terrain models along Hunter Mountain Fault Zone.

## Purpose

- Show how lidar data can be used to analyze the geomorphic evolution within the active tectonic setting of the Death Valley extended area.

- DEM derived terrain models will be used to identify fault traces from offset channels and other topographic features.

- An average lateral displacement for the fault through the study area will be measured and discussed in relation to previous studies for the region.

# Mapping offset channels from LiDAR derived terrain models along Hunter Mountain Fault Zone.

## Contents

# Panamint Valley Regional Setting

- Within the Eastern California Shear Zone (ECSZ), a N-S oriented, 100-km wide belt of right-lateral strike shearing at ~13mm/yr.

- Accommodates about 20-25% of relative plate motion between Pacific and North American plates (Miller, et al. 2001; Frankel, et al. 2007; McAuliffe, et al. 2013).

- Research focused here to understand the kinematics of the diffuse P/NA plate margin.

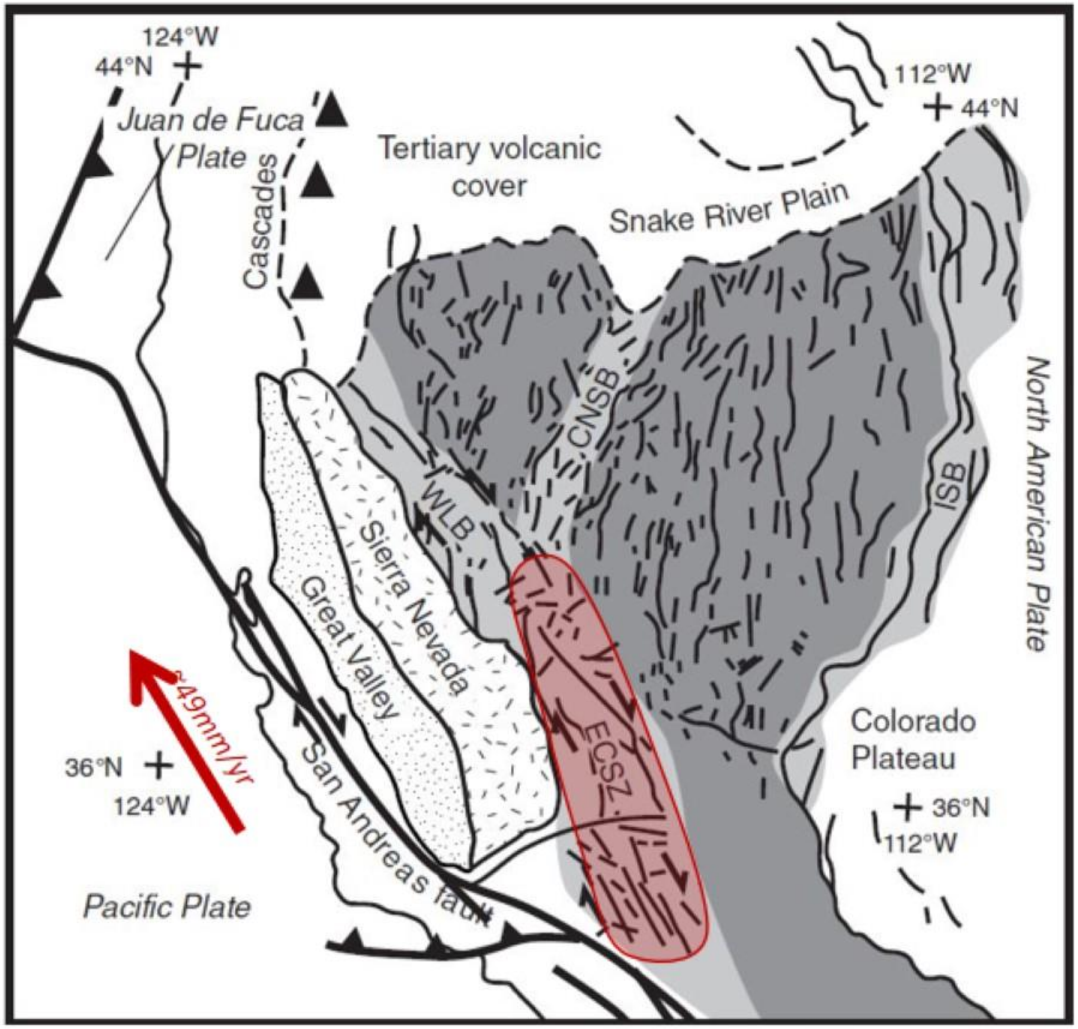


*Map of Western U.S. Cordillera tectonics with Eastern California Shear Zone highlighted in red. (Modified after Lee et al., 2006)*

## Panamint Valley Tectonics

- Development since ~15 Ma along a low-angle detachment fault system that links extension with the Death Valley Fault System (McAuliffe, et al, 2013).
- Since ~4 Ma, right-lateral, strike-slip motion has dominated the Hunter Mountain Fault Zone *(Burchfiel et al., 1986).*

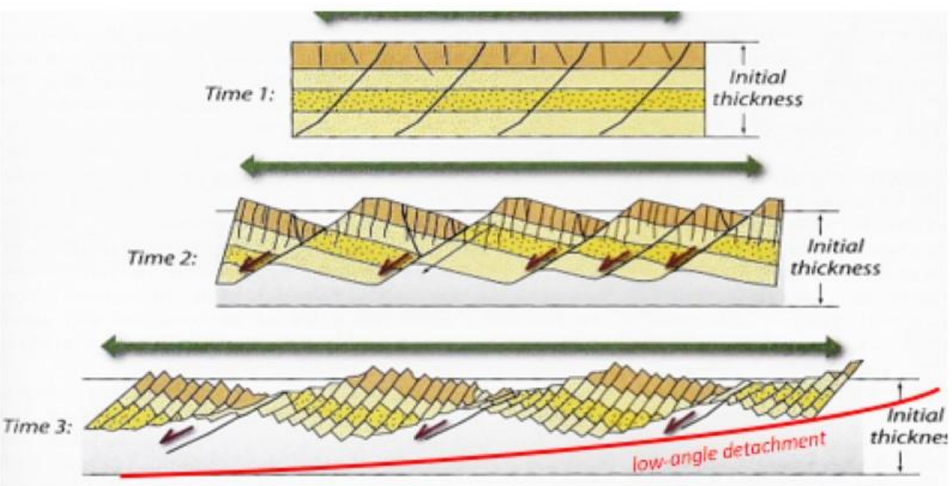


*(modified after Bierman and Montgomery, 2014)*

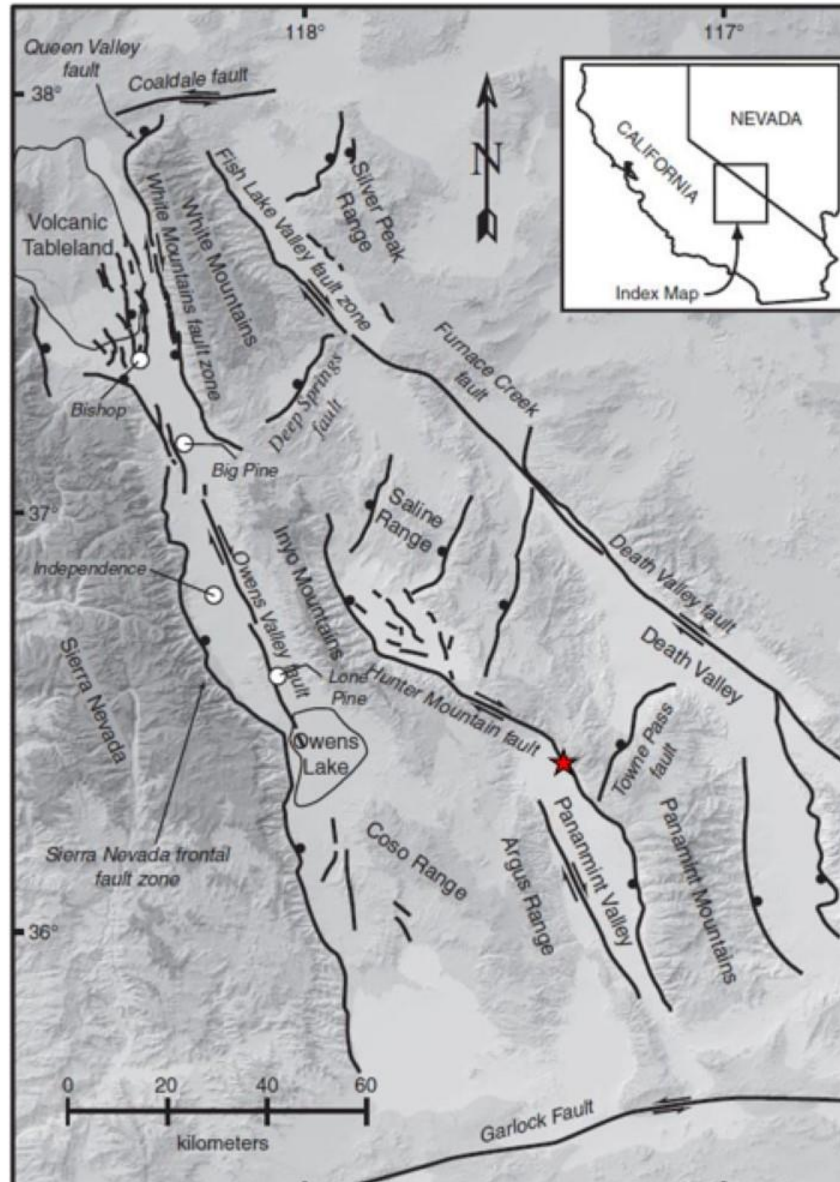


*Regional tectonic fault map of Death Valley extended area. Study area marked by red star. (Modified after Lee et al., 2006)*

# Panamint Valley Tectonics

- ~2-3.2 mm/y estimated for HMFZ from 8-10 km of offset for the ~3.0 MA Hunter Mountain Batholith. (Burchfiel et al., 1986).

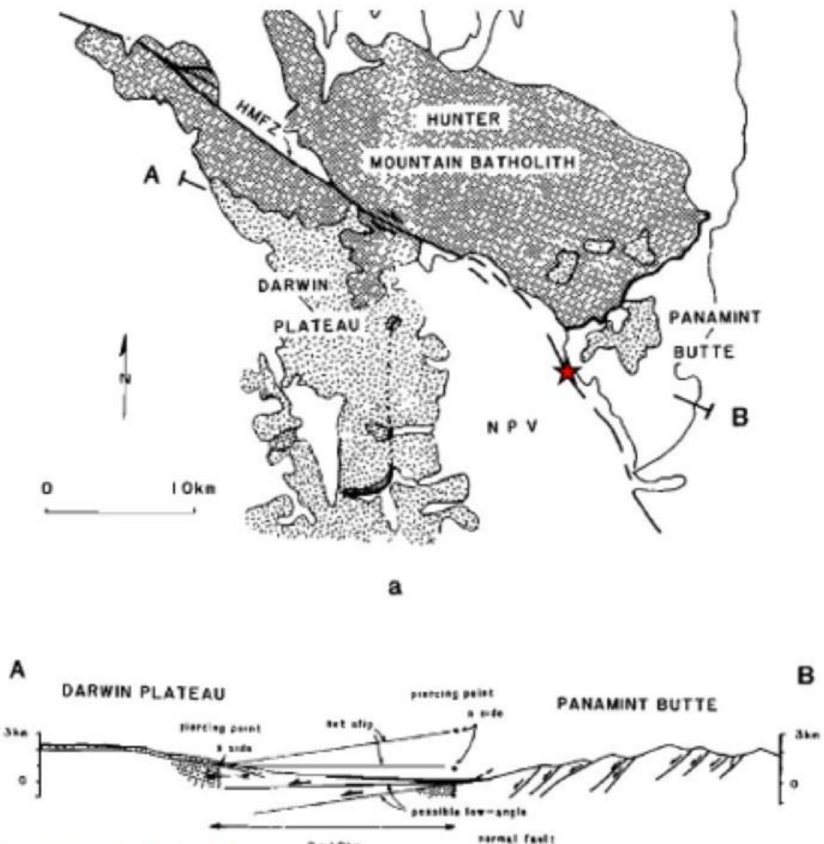


(Burchfiel et al., 1986)

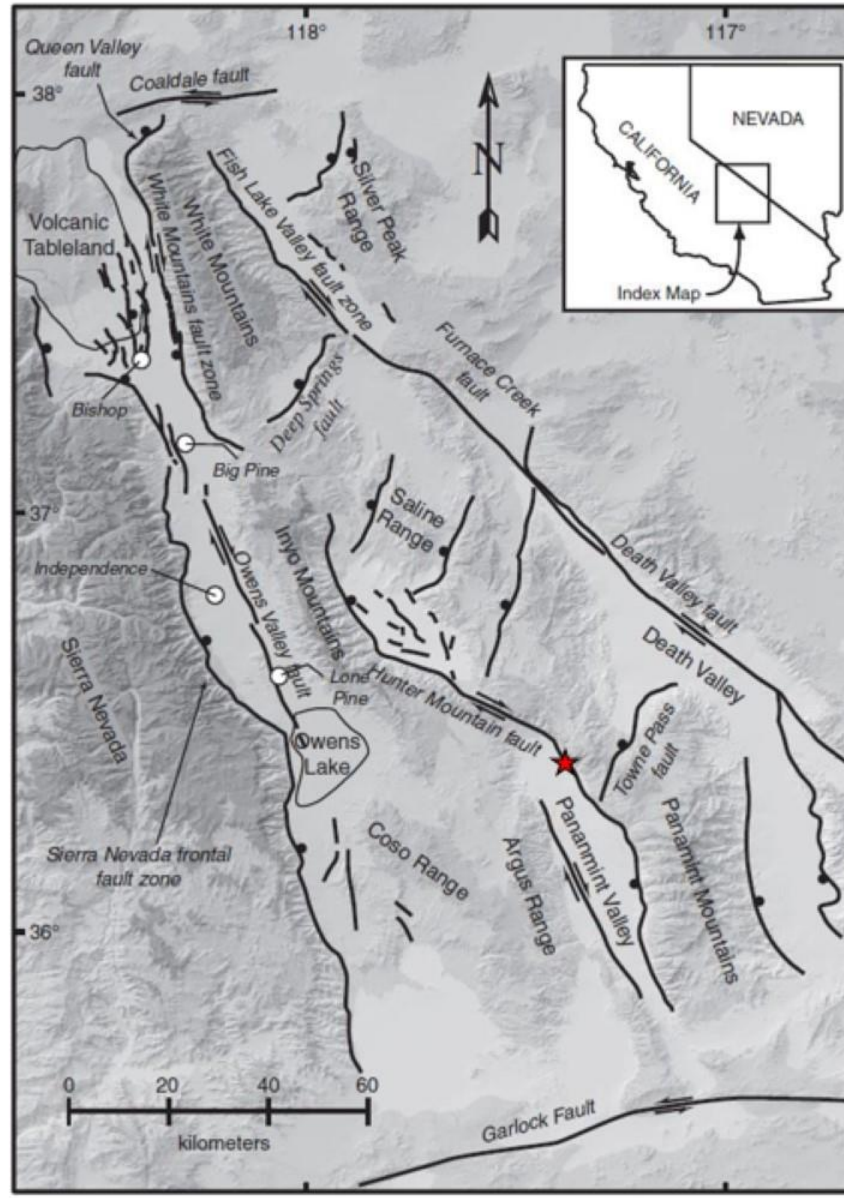


*Regional tectonic fault map of Death Valley extended area. Study area marked by red star. (Modified after Lee et al., 2006)*

## Strike- Slip Geomorphology

- Geomorphic features produced by lateral movement include:

  -Linear valley or trough

  **-Offset drainage channels**

  -Scarps

  -Abandoned or “beheaded” streams

*Offset channel in Northern Death Valley. (Randol, 2015)*

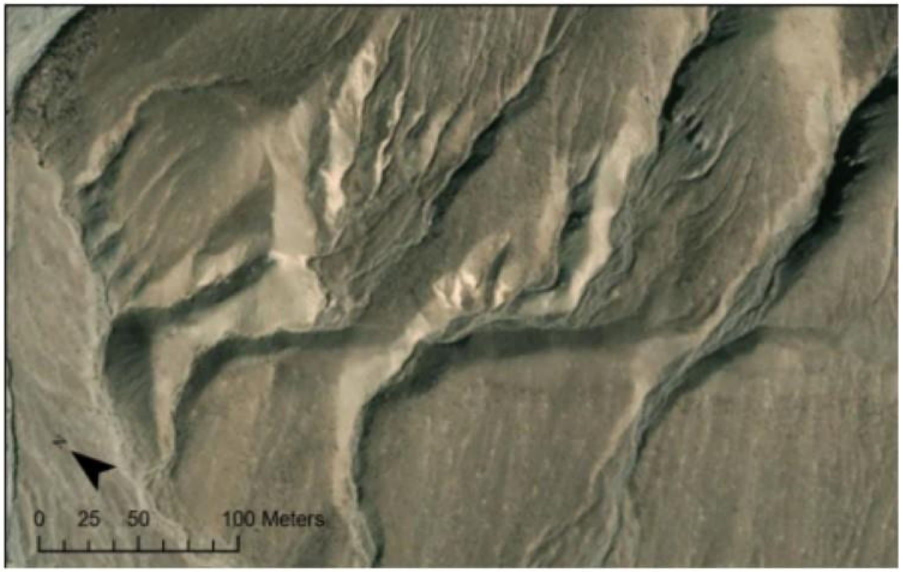


*Natural color image of study area from ESRI, Geoeye, EarthStar Geographics*

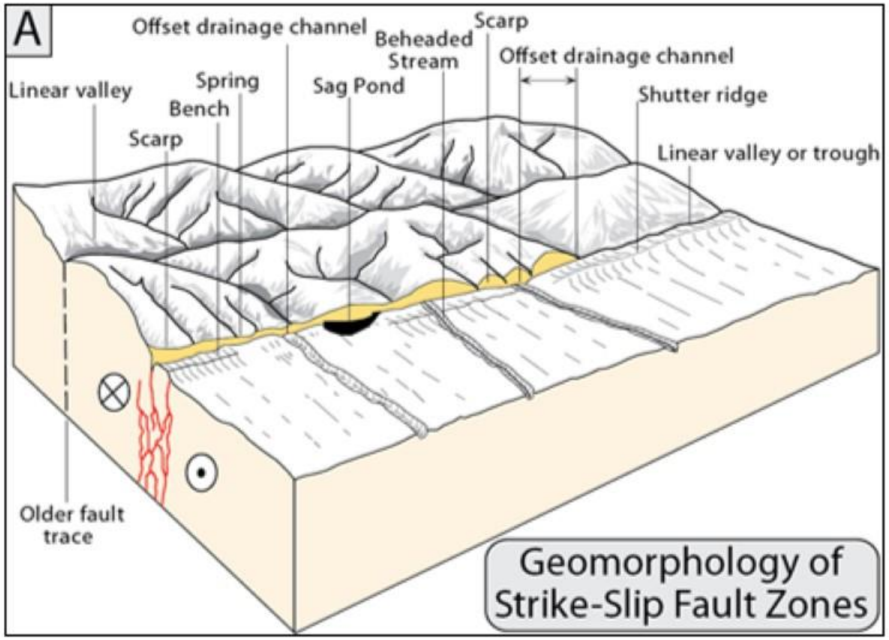


*(Modified after Burbank and Anderson, 2001)*

## LiDAR Data Source

- Point cloud data were obtained from OpenTopography.com for a 0.8 x 1.0 km study area.
- Provided to EarthScope's Plate Boundary Observatory by the National Center for Airborne Laser Mapping (NCALM).
- Program of the Nation Science Foundation (NSF) between 2003-2018.

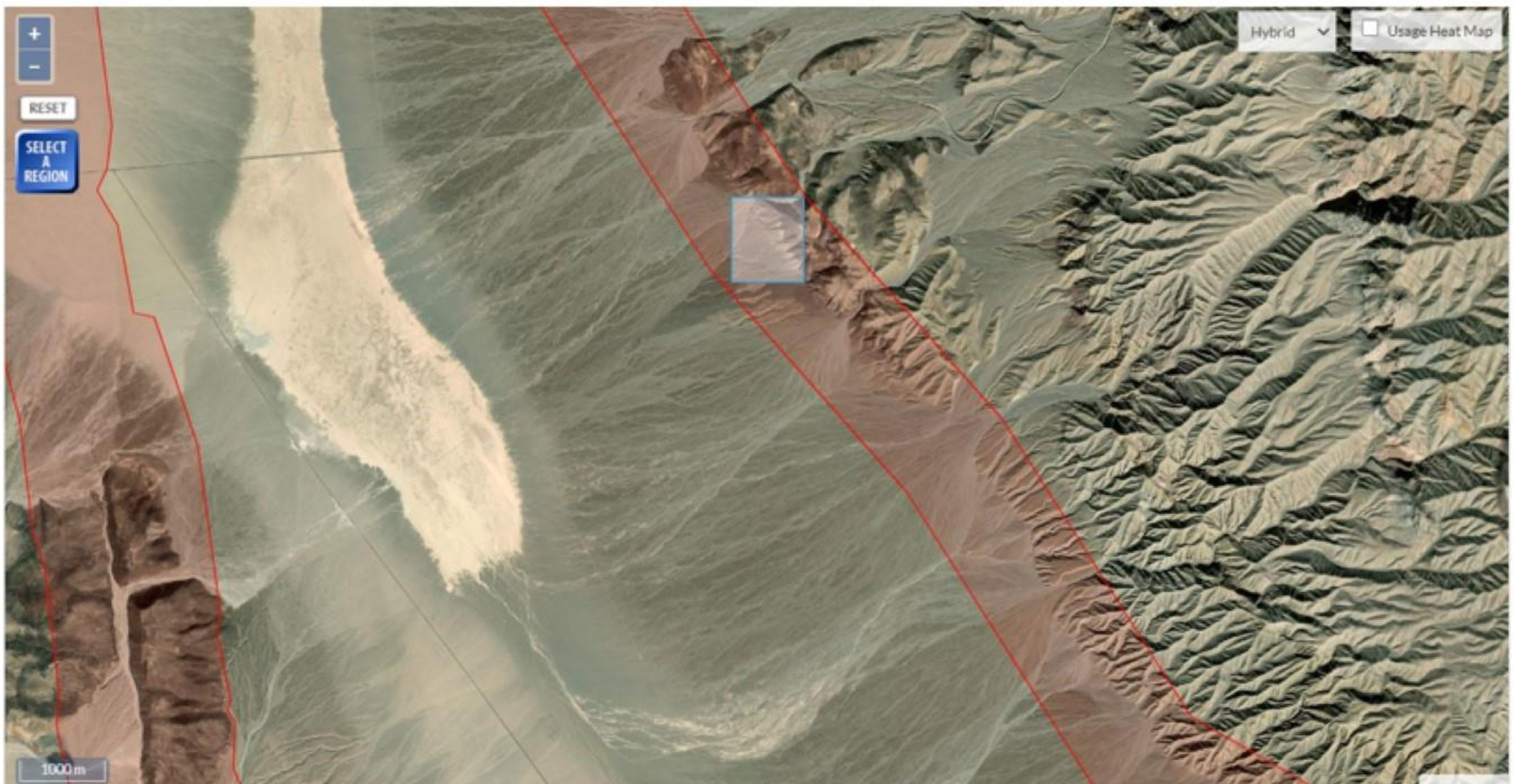


Screenshot of OpenTopography map window highlighting 2007 NCALM flight path.

## LiDAR Data Source

- The segment of the flight mission took place on April 18th in 2007.
- Optech GEMINI Airborne Laser Terrain Mapper (ALTM) mounted to twin-engine Cessna Skymaster

➢ scan frequency of 50 Hz

➢ scan angle of 11.3 degrees

➢ average point density of 4.61 pts/$m^2$.

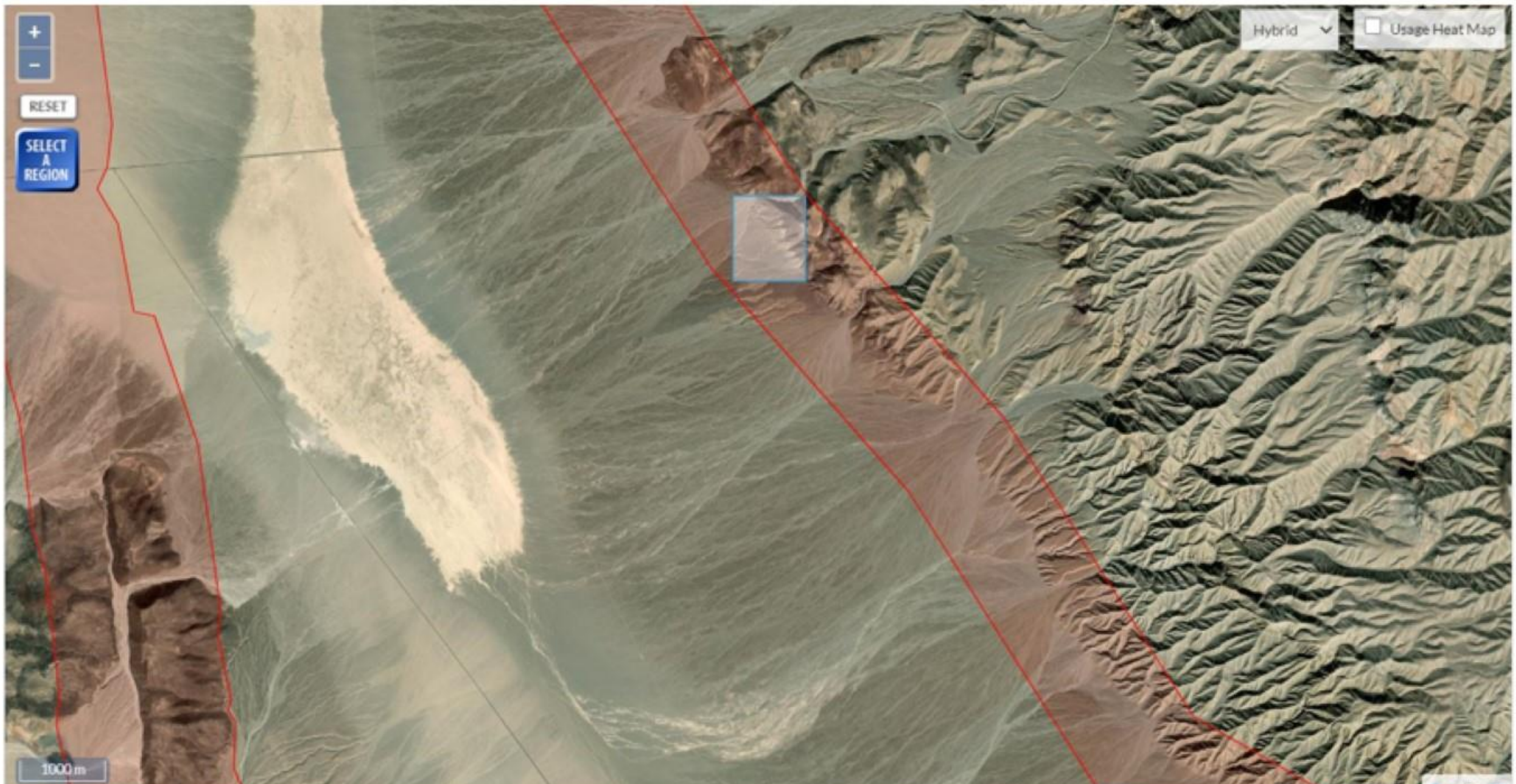


Screenshot of OpenTopography map window highlighting 2007 NCALM flight path.

## Processing Point Cloud Data

- OpenTopography LAZ format to LAS Dataset.
- Default settings in ArcGIS tools.

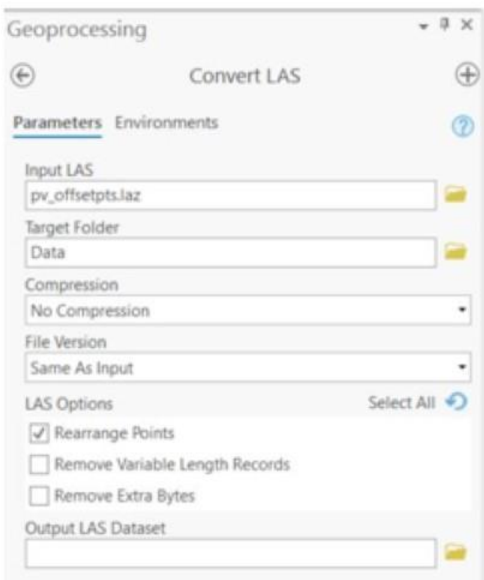


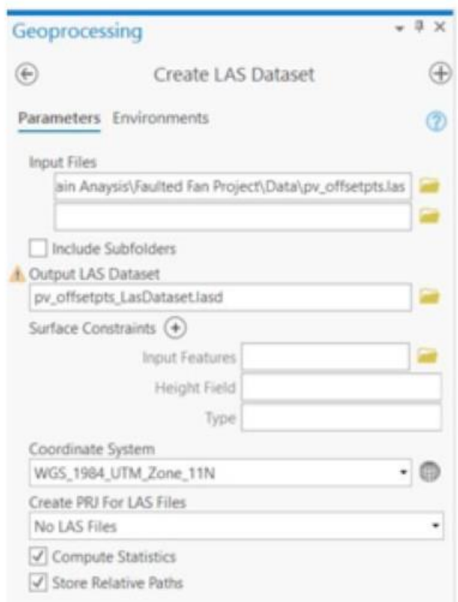


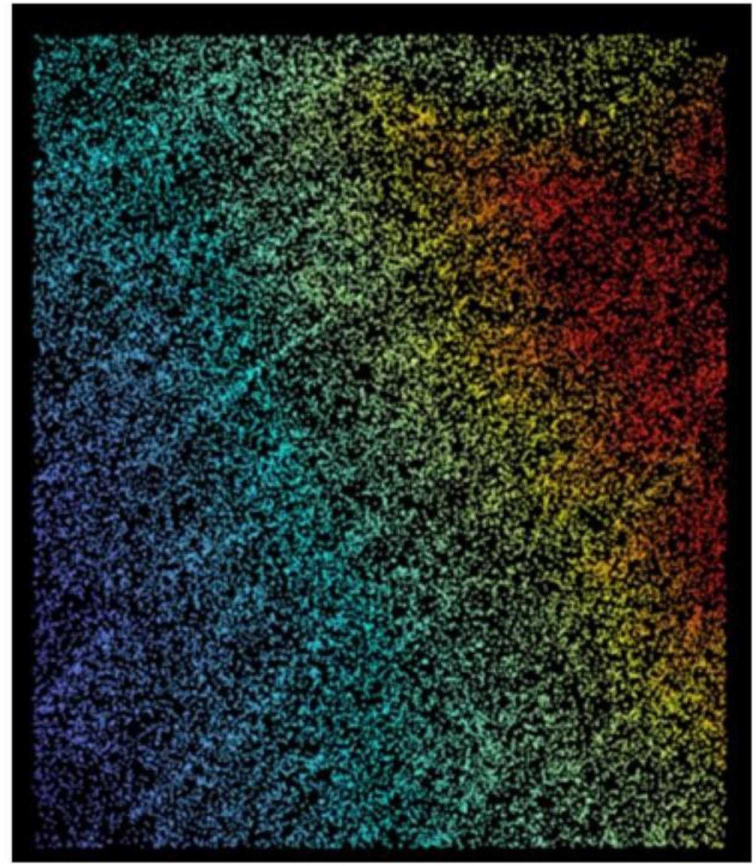

- Ground points LAS filter

# Processing Point Cloud Data

- LAS to Raster Tool
- Minimum cell assignment
- Linear void fill

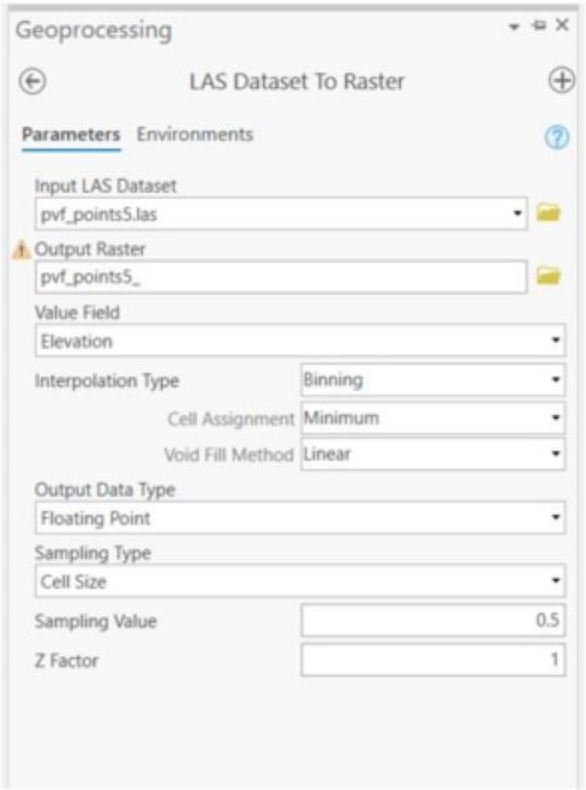


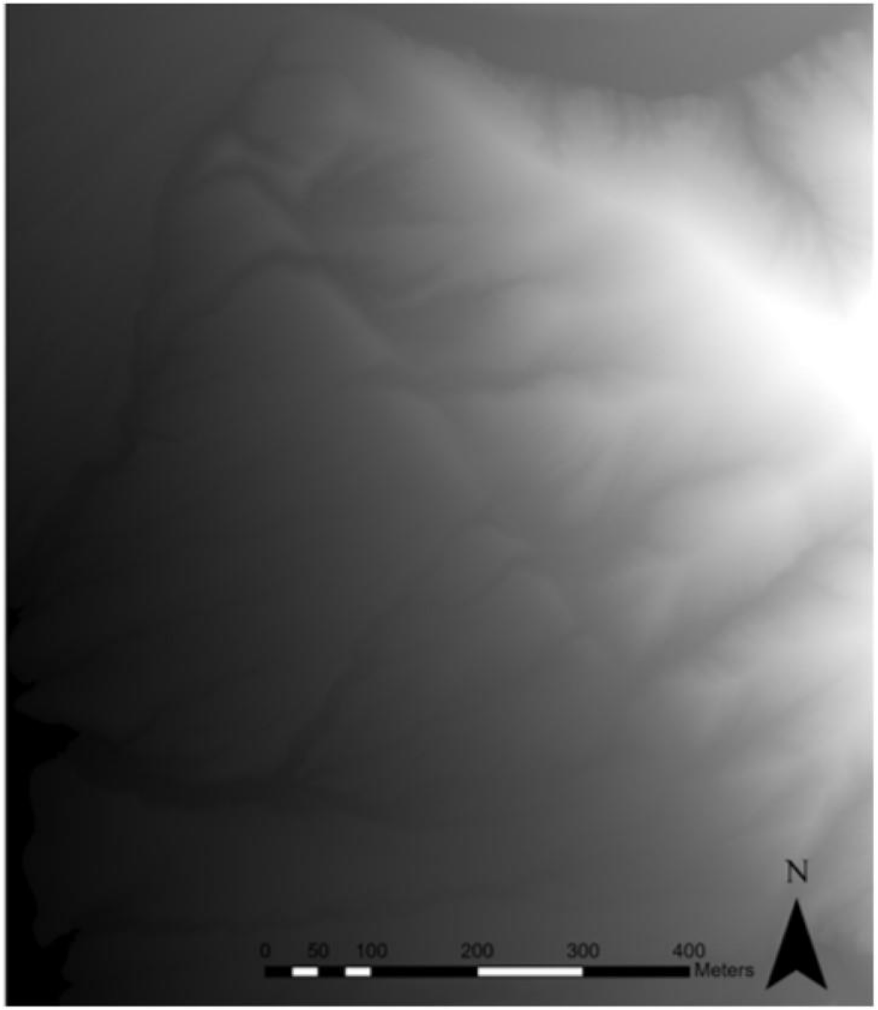


- 0.5-meter DEM generated from last return, ground points.

**Derived Terrain Models from DEM**

- All maps derived from ½ meter DEM using ArcGIS Pro **Raster Functions**.

1. Hillshade

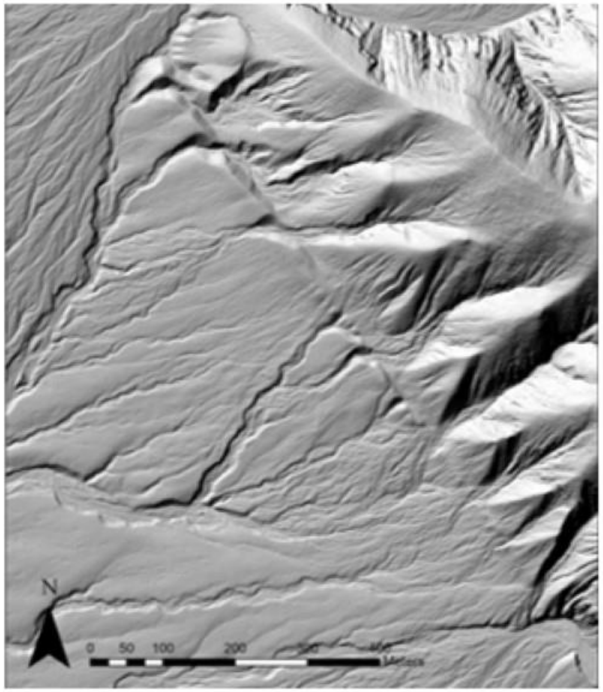


2. Slope-aspect

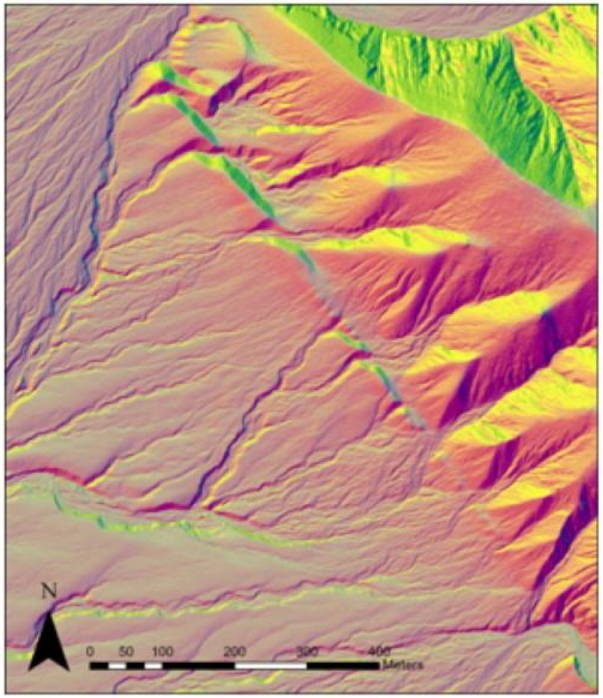


3. Shaded relief with Contours

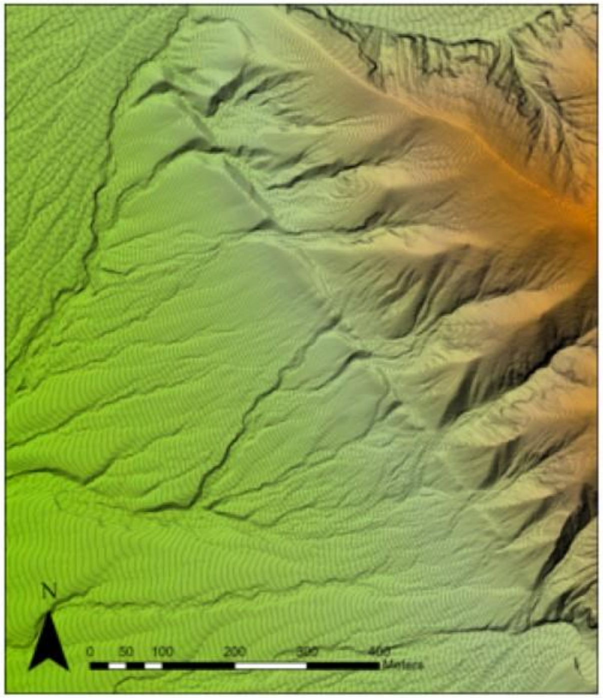

## Tracing Fault in 2D View

- Linear scarps and channel inflection points used to identify trace.
- Breaks in fault trace where active channels cover surface expression.

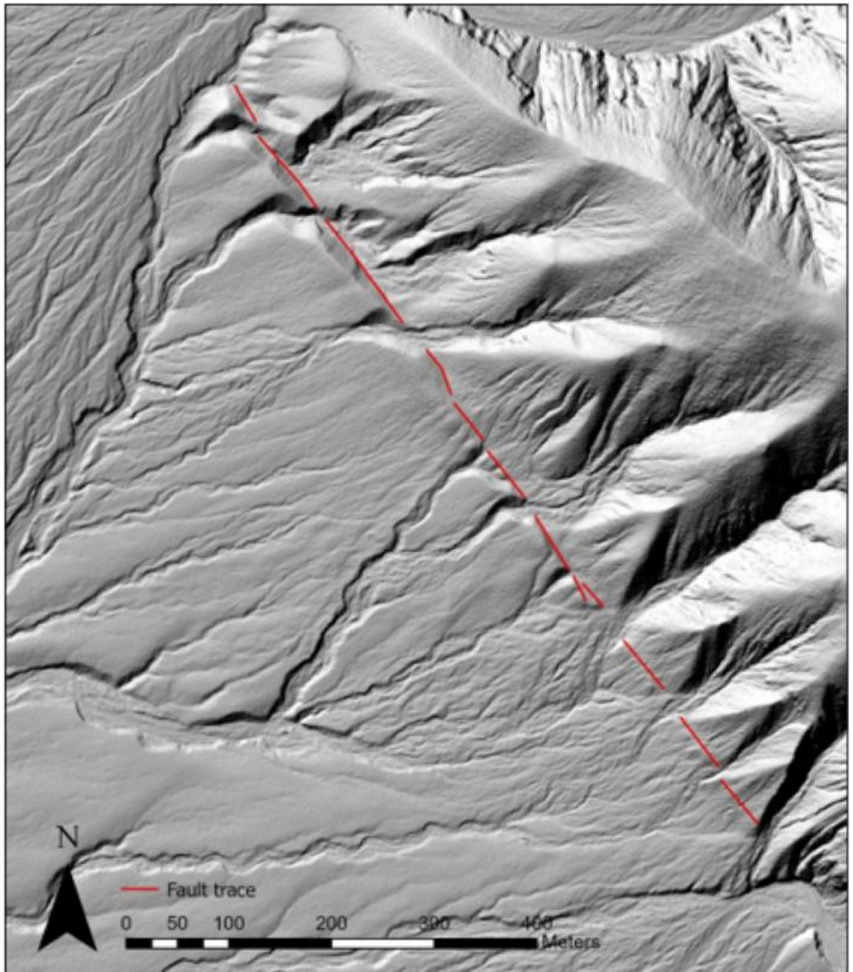


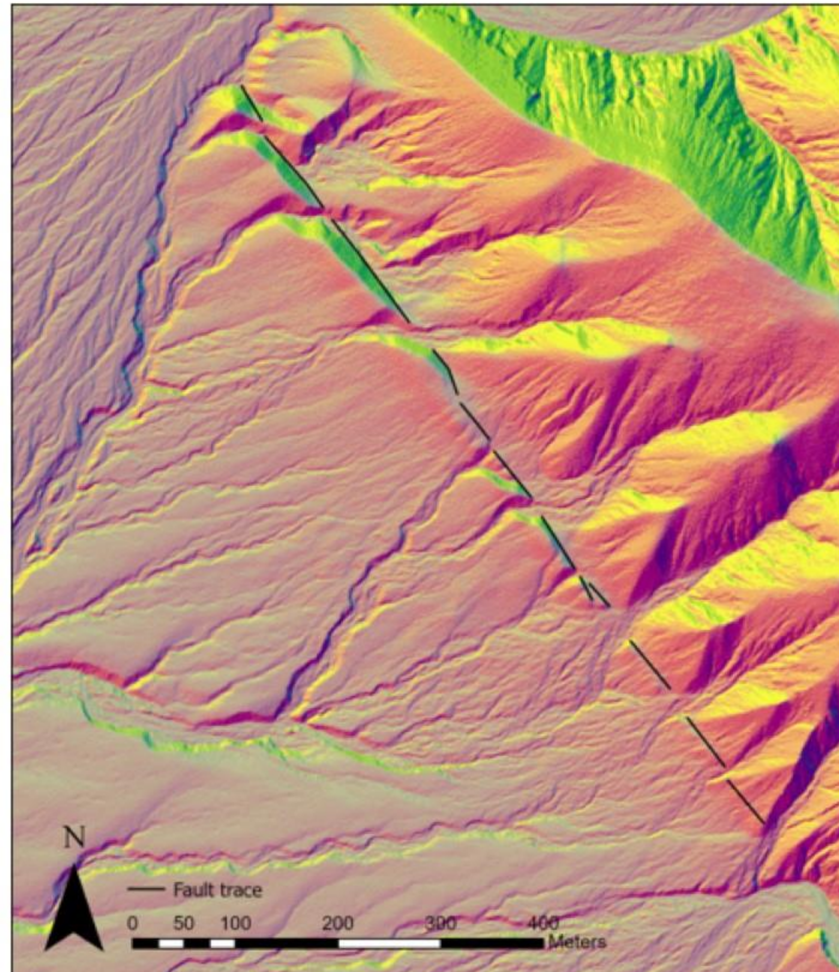

## Adjusting Fault Trace in 3D Local Scene

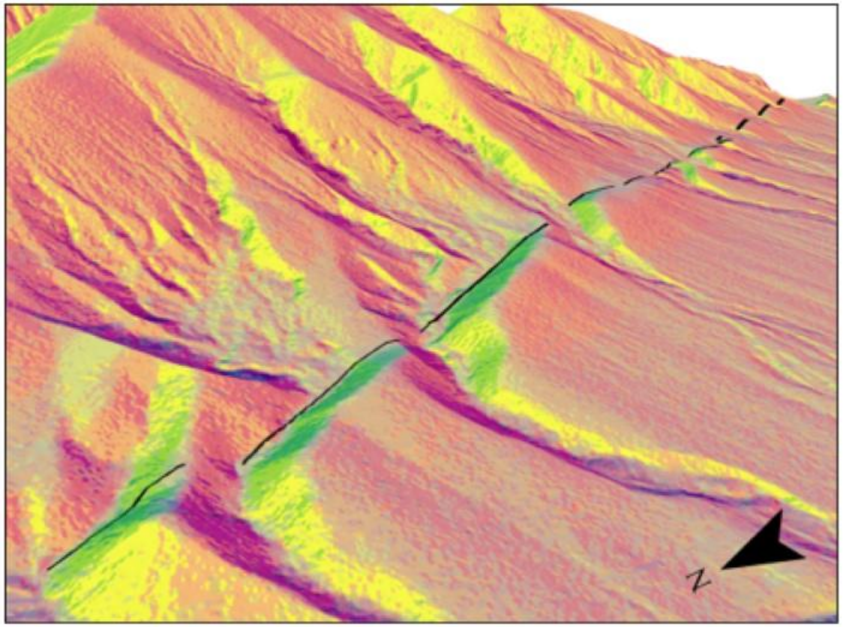


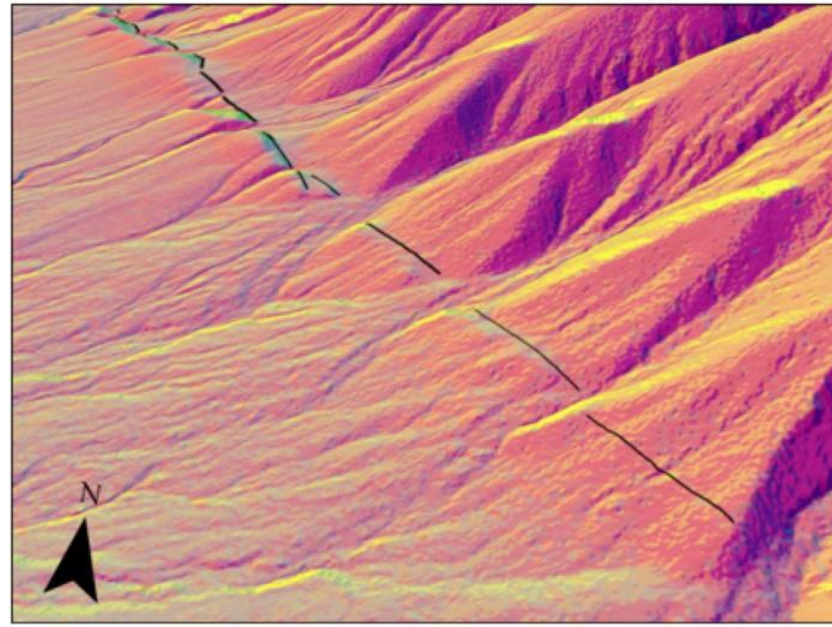


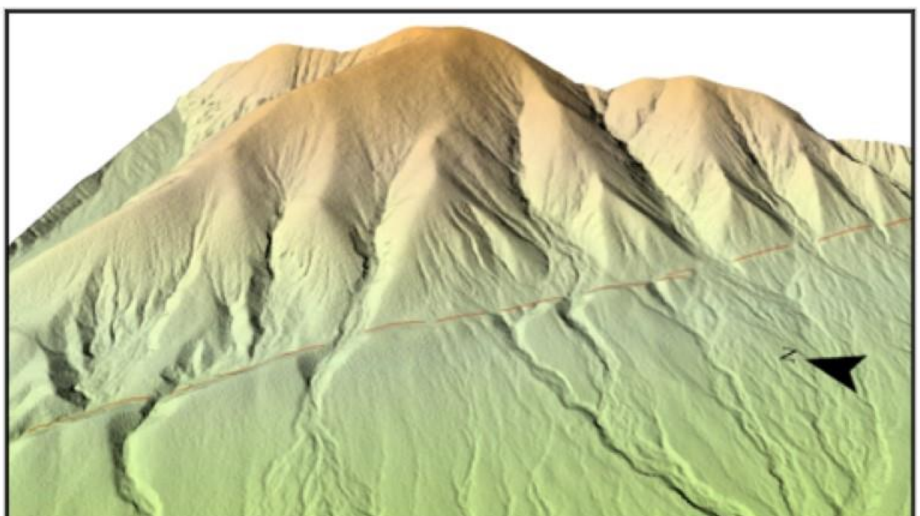


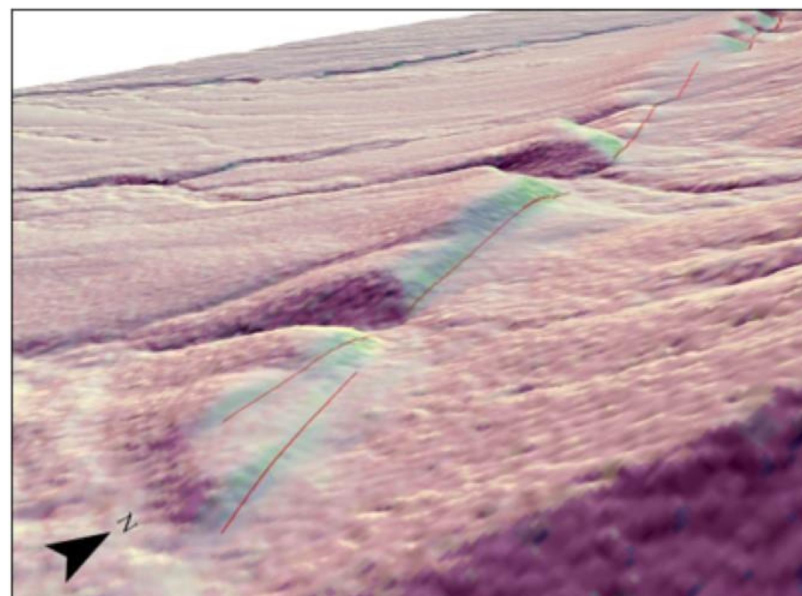

## Channel Delineation

- Watershed Delineation workflow in Raster Functions.
- Channel thalwegs extracted from stream order raster

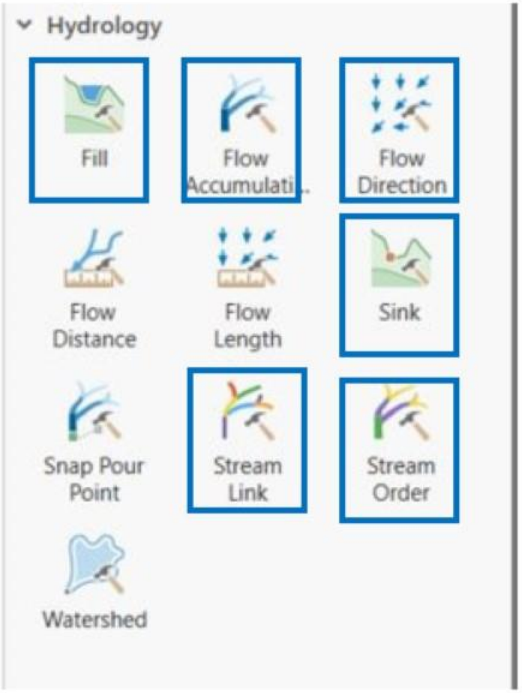


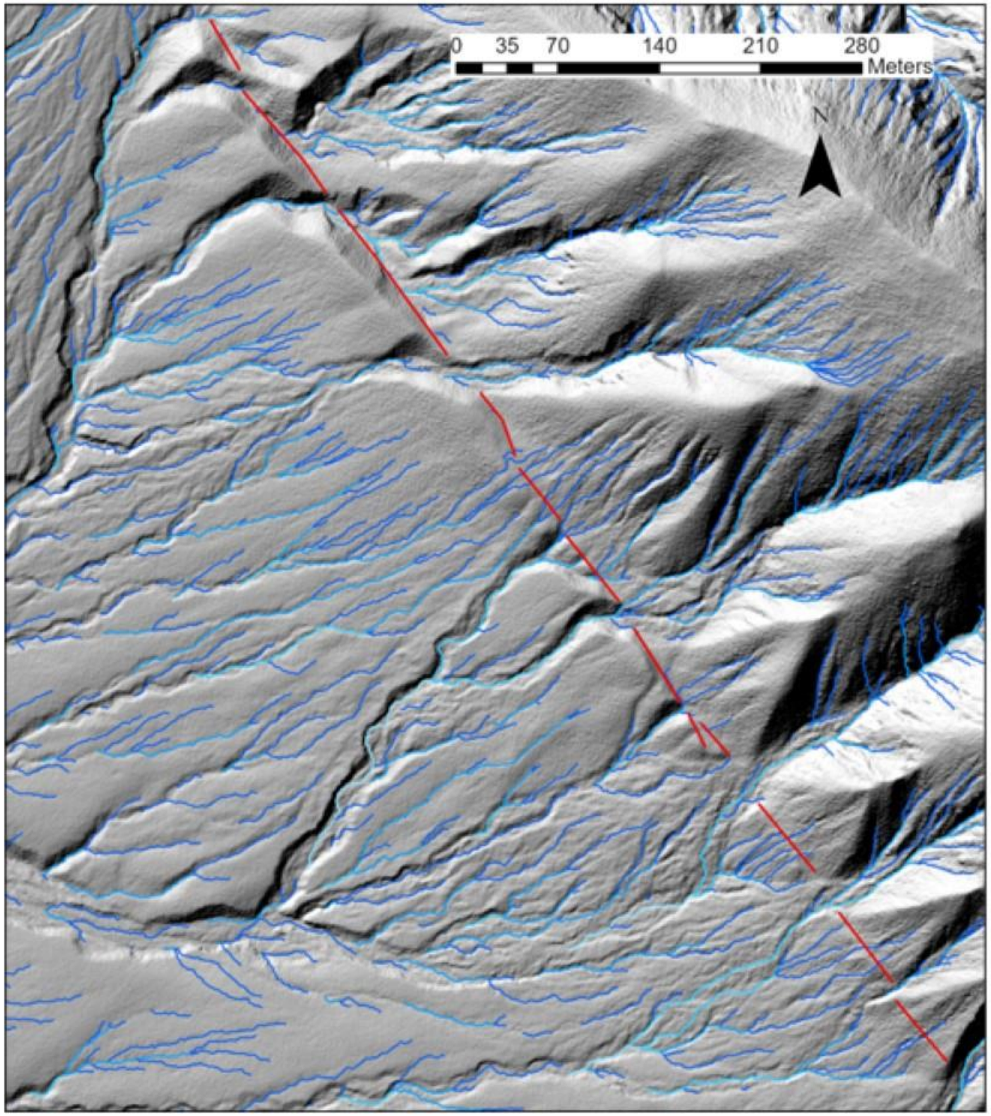

## Results: Offset Measurement

- Five channels were delineated.
- ArcGIS's Distance Measure tool.

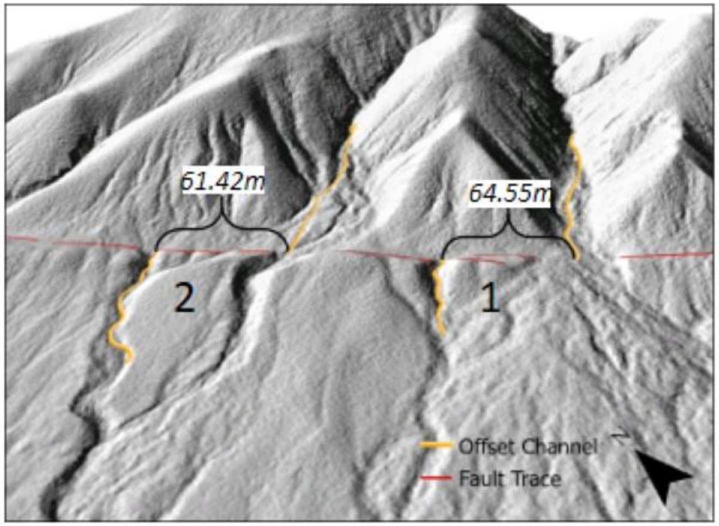


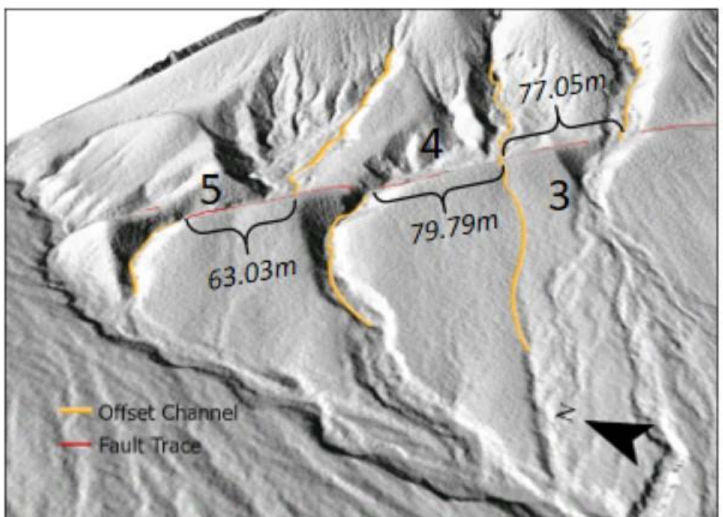


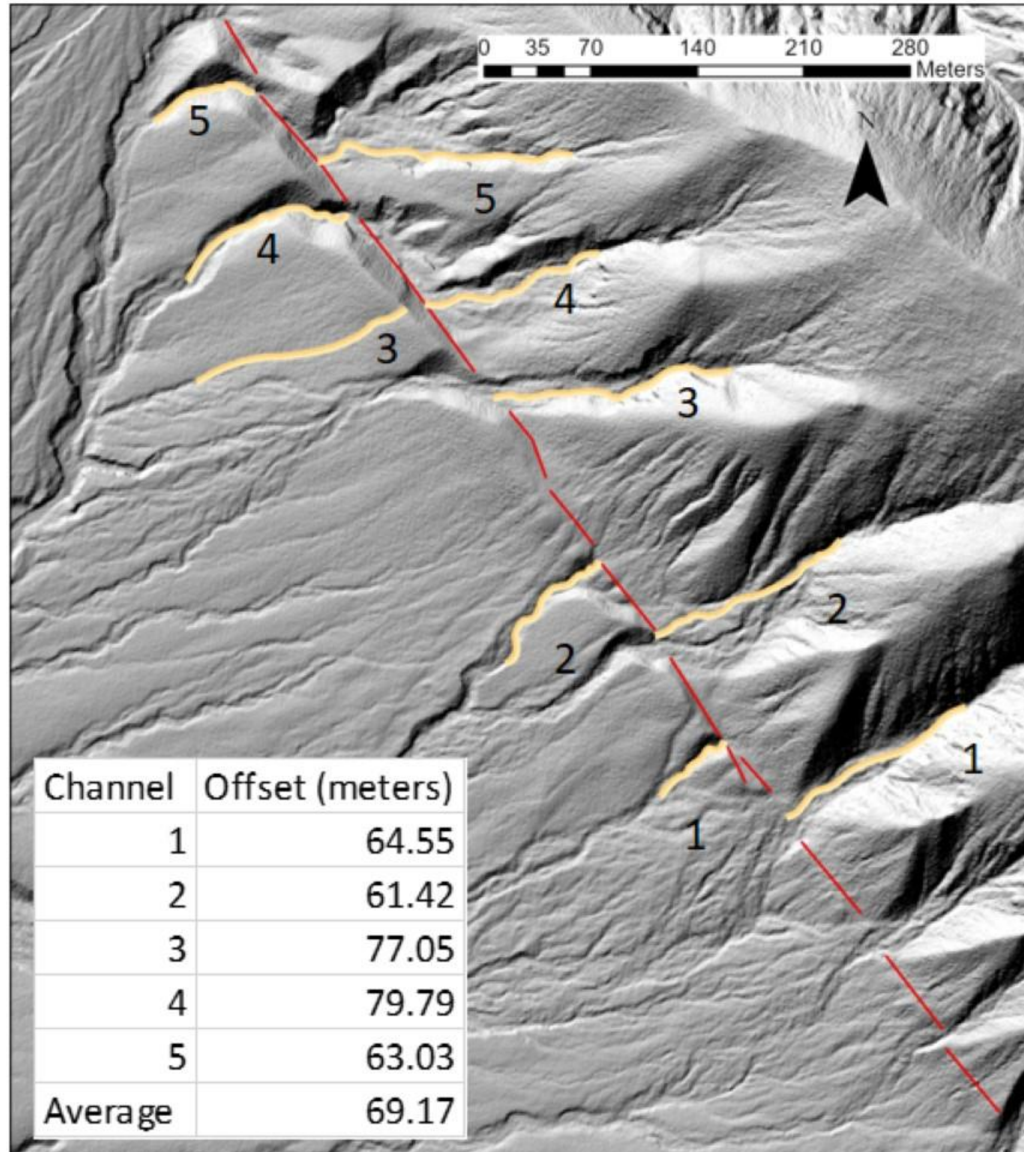


| Channel | Offset (meters) |
|---|---|
| 1 | 64.55 |
| 2 | 61.42 |
| 3 | 77.05 |
| 4 | 79.79 |
| 5 | 63.03 |
| Average | 69.17 |

**Results: Derived Terrains**

- Slope-Aspect draped over the Hillshade highlighted the surface trace of the fault more clearly than others.

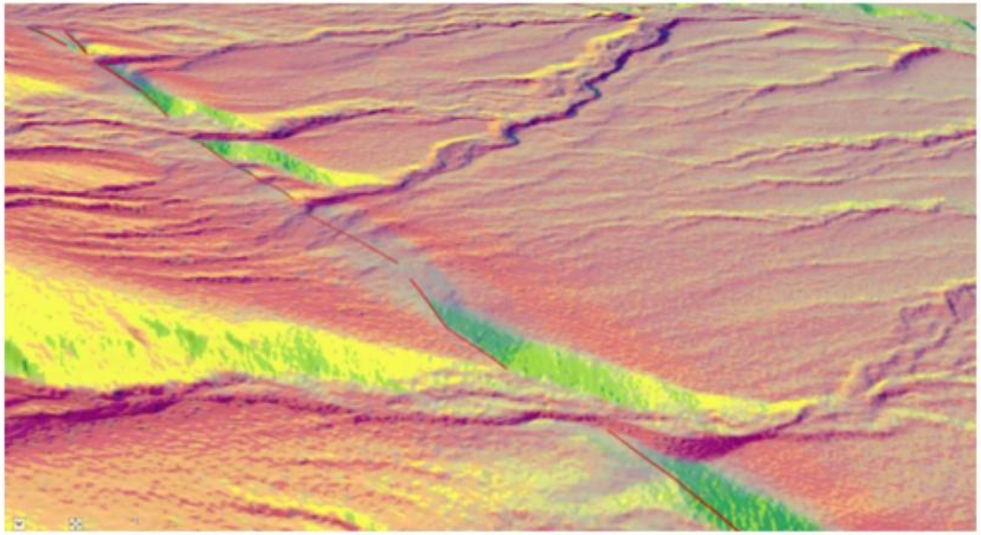

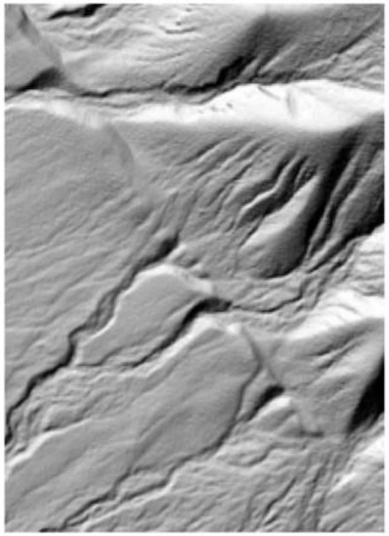

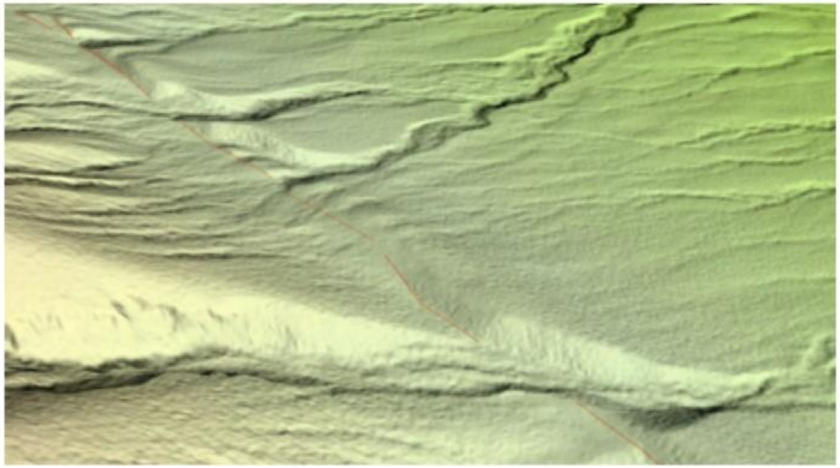

- 3D Scene more effective for identifying geomorphic landforms related to faulting.
- Sense of field observations.

**Results: Thalweg Delineation**

- Stream links and stream order rasters helped to identify active channel centers.
- Highlighting subtle abandoned stream segments invisible to aerial or satellite natural color images.

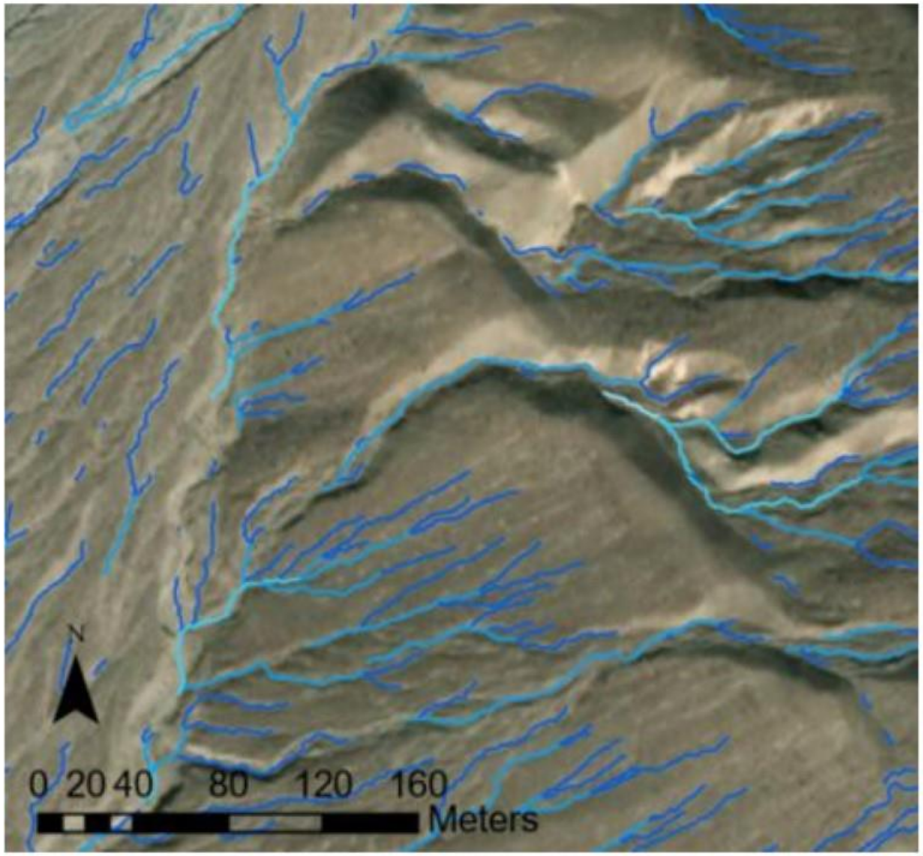


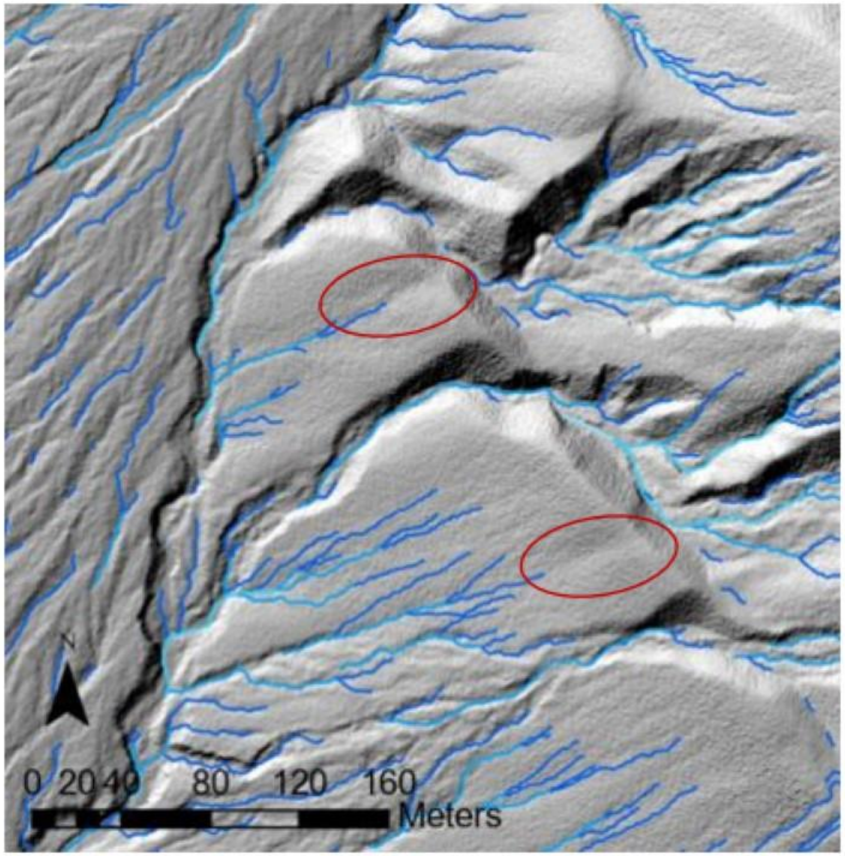

**Discussion/Conclusion**

- Without an age estimate for the study area fan surface or channel abandonment, a meaningful slip rate cannot be estimated.
- If slip through this segment of the HMFZ is consistent with the 2-3.2 mm/yr
- Age of the pre-faulted, alluvial fan between 25 and 34 ka.

$$\frac{\sim 69\text{m}}{2\text{-}3.2\ \text{mm/yr}} \approx 25\text{-}34\ \text{ka}$$

## Discussion/Conclusion

- The method for this type of study has been greatly scaled back and generalized to provide more of an overview for fault analysis from LiDAR.

- A more complete tectonic evolution and slip rate study would include:

  -fan surface age constraints

  -stream channel profiles across fault

  -in-depth statistical analysis for accuracy of measurements and potential error.

# Discussion/Conclusion

## Time-predictable model application in probabilistic seismic hazard analysis of faults in Taiwan

Yu-Wen Chang[1,2], Chin-Hsiung Loh[2,*], and Wen-Yu Jean[1]

[1] *National Center for Research on Earthquake Engineering, National Applied Research Laboratories, Taipei City, Taiwan*
[2] *Department of Civil Engineering, National Taiwan University, Taipei City, Taiwan*

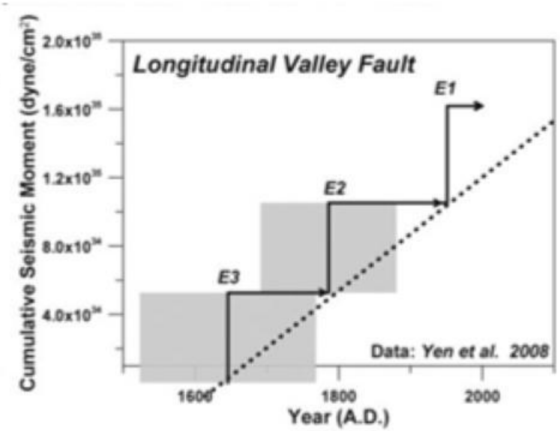


the recurrence interval for each event

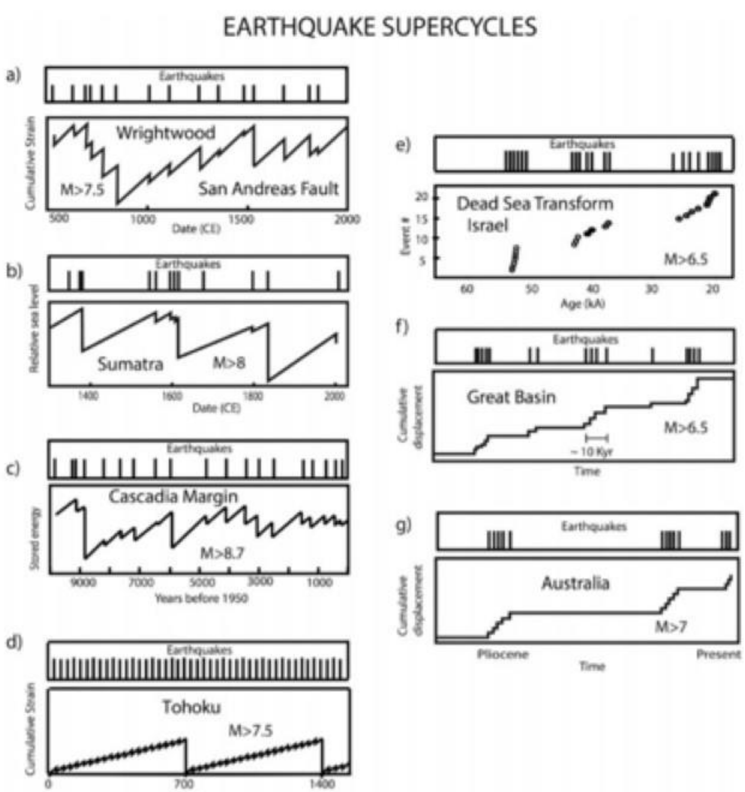


## Earthquake supercycles and Long-Term Fault Memory

Leah Salditch[a,b,*], Seth Stein[a,b], James Neely[a], Bruce D. Spencer[b,c], Edward M. Brooks[a,b], Amotz Agnon[d], Mian Liu[e]

[a] *Department of Earth and Planetary Sciences, Northwestern University, 2145 Sheridan Rd., Evanston, IL 60208, USA*
[b] *Institute for Policy Research, Northwestern University, 2040 Sheridan Rd., Evanston, IL 60208, USA*
[c] *Department of Statistics, Northwestern University, 2006 Sheridan Rd., Evanston, IL 60208, USA*
[d] *Institute of Earth Sciences, Hebrew University, Sderot Magnes, Jerusalem 9190401, Israel*
[e] *Department of Geological Sciences, University of Missouri, 101 Geological Sciences Bldg., Columbia, MO 65211, USA*

## References

B.C. BURCHFIEL, K. V. HODGES AND L. H. ROYDEN (1986), Geology of Panamint Valley - Saline Valley Pull-Apart System, California: Palinspastic Evidence of or Low-Angle Geometry of a Neogene Range-Bounding Fault, JOURNAL OF GEOPHYSICAL RESEARCH, VOL. 92, NO. B10, PAGES 10,422-10,426, SEPTEMBER 10, 1987

Bull, W. B. (1977), The alluvial fan environment, Prog. Phys. Geogr., 1, 222–270.

Frankel, K.L., Dolan, J.F., Owen, L.A., Finkel, R.C., and Hoeft, J.S., (2007), Spatial variations in slip rate along the Death Valley-Fish Lake Valley fault system from LiDAR topographic data and cosmogenic 10Be geochronology: Geophysical Research Letters, v. 34, doi:10.1029/2007GL030549.

Klinger, R. E. (2002), Quaternary stratigraphy and geomorphology of northern Death Valley - Implications for tectonic activity along the northern Death Valley fault, Ph.D. dissertation, 312 pp., Univ. of Colo., Boulder.

Lee, J., Stockli, D., Schroeder, J., Tincher, C., Bradley, D., Owen, L., Gosse, J., Finkel, R., and Garwood, J., (2006), Fault slip transfer in the Eastern California Shear Zone–Walker Lane Belt: Geological Society of America Penrose Conference Field Trip Guide (Kinematics and Geodynamics of Intraplate Dextral Shear in Eastern California and Western Nevada, Mammoth Lakes, California, 21–26 April 2005), 26 p., doi: 10.1130/2006.FSTITE.PFG.

McAuliffe, L. J., Dolan, J. F., Kirby, E., Rollins, C., Haravitch, B., Alm, S., and Rittenour, T. M. (2013), Paleoseismology of the southern Panamint Valley fault: Implications for regional earthquake occurrence and seismic hazard in southern California, J. Geophys. Res. Solid Earth, 118, 5126– 5146, doi:10.1002/jgrb.50359.

Miller, M. M., Johnson, D. J., Dixon, T. H., and Dokka, R. K. (2001), Refined kinematics of the eastern California shear zone from GPS observations, 1993–1998, J. Geophys. Res., 106( B2), 2245– 2263, doi:10.1029/2000JB900328.

Oskin, M. E., K. Le, and M. D. Strane (2007), Quantifying fault-zone activity in arid environments with high resolution topography, Geophys. Res. Lett., 34, L23S05, doi:10.1029/2007GL031295

Regmi, N. R., E. V. McDonald, and S. N. Bacon (2014), Mapping Quaternary alluvial fans in the southwestern United States based on multiparameter surface roughness of lidar topographic data, J. Geophys. Res. Earth Surf., 119, 12–27, doi:10.1002/2012JF002711.

Zhang, P., Ellis, M.A., Slemmons, D.B., Mao, F., 1990. Rightlateral displacements associated with prehistoric earthquakes and Holocene slip rate along the southern Panamint Valley fault zone: implications for southern Basin and Range tectonics. J. Geophys. Res. 95, 4857 – 4872.

***Lidar point cloud (.LAZ)***

*This material is based on services provided to the Plate Boundary Observatory by NCALM (http://www.ncalm.org). PBO is operated by UNAVCO for EarthScope (http://www.earthscope.org) and supported by the National Science Foundation (No. EAR-0350028 and EAR-0732947*